

Chapter 3

Modeling of Maximum Power Point Tracking for Stand-Alone PV Systems



3.1 Introduction

The PV systems utilize semiconductor materials and electronic technology to convert the incident sunlight into electricity. At the heart of the PV system is the PV cell, a semiconductor material which generates electrical voltage and/or current when exposed to the solar irradiance. The PV cells generate electricity via the PV effect, in which semiconductor holes and electrons freed by photons from the incident solar irradiance are dragged to opposite terminals of the PV cell by the resulting electric field [6]. The PV cell generates a specified power according to its current-voltage (I-V) and power-voltage (P-V) characteristics. Thus, the PV cells must be aggregated together to produce enough current and voltage for practical applications. In this regard, a PV module is formed by connecting several PV cells in series; the PV modules are connected in series to form a PV string. The PV strings, in turn, are connected in parallel to form a PV array in order to generate adequate voltage and power to be integrated with the electrical grid.

The incident solar irradiance on the PV array varies due to various reasons such as the variation of time in a day, the atmospheric effects such as clouds, and the latitude of the location. Therefore, the MPPT techniques are implemented to regulate the output voltage and current of PV array for extraction of the maximum power during variation of the solar irradiation. In addition, the PV systems are equipped with a DC/DC converter to implement the MPPT technique [64]. This chapter discusses the fundamental components of the stand-alone PV systems. Moreover, this chapter introduces the study and design of two techniques of MPPT that implemented in the PV conversion systems, namely, the perturb and observe (P&O) MPPT technique and the incremental conductance (InCond) MPPT technique.

3.2 Principle of PV Conversion Systems

Without pollution or greenhouse gas emission, a PV conversion system converts the sunlight directly into electricity. The basic element of a PV conversion system is the PV cell. The PV cell is basically made up of a semiconductor material (P-N junction) that able to generate the electric current when being exposed to the sunlight irradiation. Figure 3.1 illustrates the photocurrent generation principle of the PV cell. These PV modules can be grouped in series and/or parallel to form a PV array as depicted in Fig. 3.2. The PV modules are connected in parallel to increase the output current and connected in series to provide a greater output voltage.

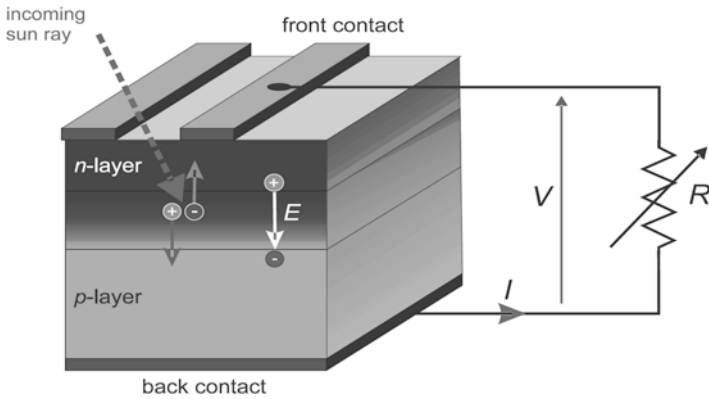


Fig. 3.1 Photocurrent generation principle of the PV cell [67]

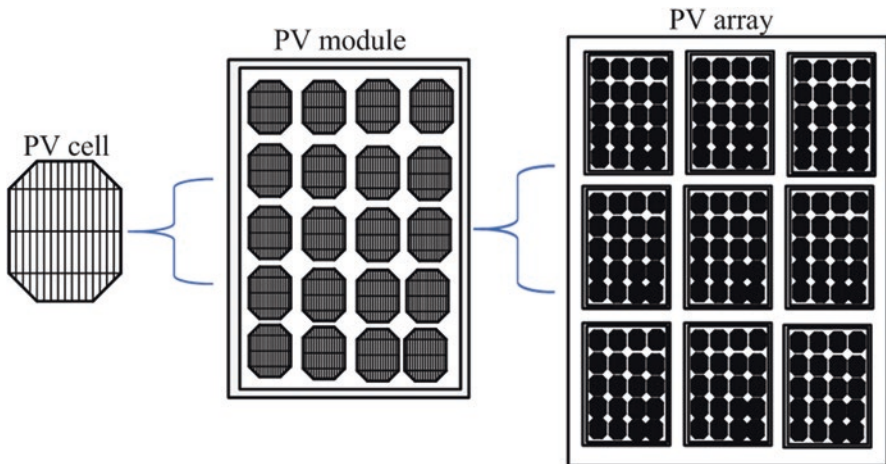


Fig. 3.2 PV cell, PV module, and PV array [67]

The dynamic performance of the PV conversion systems depends on the design quality of the PV cells and the operating conditions. The major families of PV cells include monocrystalline technology, polycrystalline technology, and thin-film technology. The monocrystalline and polycrystalline technologies are based on micro-electronic manufacturing technology and their efficiency generally between 9% and 12% for polycrystalline and between 10% and 15% for monocrystalline. For the thin-film technology, the efficiency for $CdTe$ is 9%, 10% for $a - Si$, and 12% for $CuInSe_2$ [65]. Therefore, the monocrystalline PV cells are the most employed in the PV systems since they have the highest efficiency. Moreover, the electrical characteristics of PV array such as the output voltage, current, and power vary according to the changes of the environmental conditions such as the solar irradiance and the temperature. Therefore, the effect of the environmental condition's variations must be considered in the design of PV array so that any change in the solar irradiance or temperature should not adversely affect the output power of PV array [66].

3.3 The Main Components of Stand-Alone PV Systems

The Simulink block diagram of a stand-alone PV system is manifested in Fig. 3.3. The fundamental element of a stand-alone PV system is the PV array, which converts the solar energy directly into the electric energy. Then, the DC/DC boost converter is employed to step up the output voltage from PV array to be compatible with the electrical loads. Moreover, the MPPT technique is implemented on the boost converter to extract the maximum power from the PV system during variation of the solar irradiance. In the following, the basic elements that employed in stand-alone PV systems are discussed in detail.

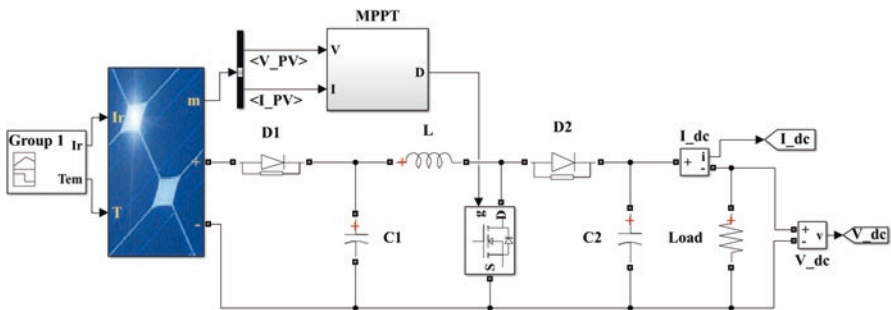


Fig. 3.3 Simulink block diagram of the stand-alone PV system with DC/DC converter

3.3.1 The Equivalent Circuit of the PV Model

The basic element of the PV conversion system is the PV cell, which is a just simple P-N junction. The equivalent circuit of the PV cell based on the well-known single-diode model is shown in Fig. 3.4. It includes the current source (photocurrent), a diode (D), series resistance (R_s) that describes the internal resistance to flow of current, and parallel resistance (R_{sh}) that represents the leakage current. The current-voltage (I-V) characteristics of the PV cell can be expressed as follows [1, 66]:

$$I = I_{ph} - I_s \left\{ \exp \left[\frac{q(V + IR_s)}{A \cdot K \cdot T} \right] - 1 \right\} - \left(\frac{V + IR_s}{R_{sh}} \right) \quad (3.1)$$

The light-generated current (I_{ph}) mainly depends on the solar irradiance and working temperature of PV cell, which is expressed as follows:

$$I_{ph} = [I_{sc} + K_i(T - T_{ref})] \cdot \left(\frac{G}{1000} \right) \quad (3.2)$$

The PV saturation current (I_s) varies as a cubic function of the PV cell temperature (T), and it can be described as follows:

$$I_s = I_{rs} \left(\frac{T}{T_{ref}} \right)^3 \exp \left[\frac{q \cdot E_g}{K \cdot A} \cdot \left(\frac{1}{T_{ref}} - \frac{1}{T} \right) \right] \quad (3.3)$$

The reverse saturation current (I_{rs}) can be approximately obtained as follows:

$$I_{rs} = \frac{I_{sc}}{\left[\exp \left(\frac{qV_{oc}}{N_{ser} \cdot K \cdot A \cdot T} \right) - 1 \right]} \quad (3.4)$$

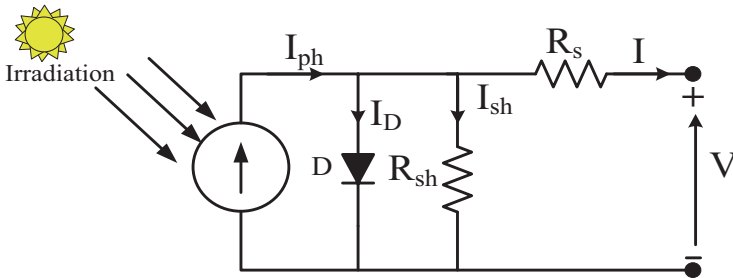


Fig. 3.4 Equivalent circuit of the PV cell

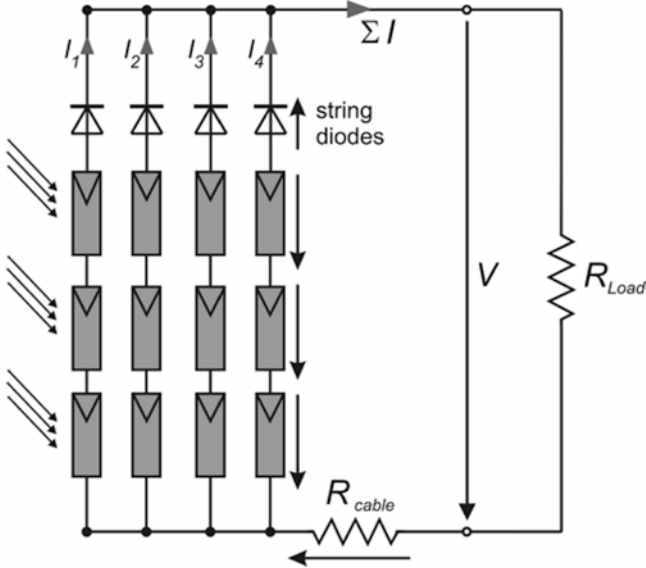


Fig. 3.5 Configuration of the PV array

The PV cell generates a specified power according to its current-voltage (I-V) and power-voltage (P-V) characteristics. Therefore, the PV cells must be aggregated together to generate sufficient current and voltage for practical applications. In this regard, a PV module is formed by connecting several PV cells in series; the PV modules are connected in series to form a PV string to provide a greater output voltage. Then, the PV strings, in turn, are connected in parallel to form a PV array to increase the output current and generate sufficient power to be synchronized with the electrical grid, as illustrated in Fig. 3.5. The electrical characteristics of PV array such as output voltage, output current, and output power can be simulated with regard to the variations of the environmental conditions such as the solar irradiance and temperature. Figure 3.6 illustrates the current-voltage (I-V) and the power-voltage (P-V) characteristics of a typical PV array during variation of the solar irradiance and temperature. As illustrated in Fig. 3.6a, the solar irradiance has a great effect on the short-circuit current (I_{sc}), while in Fig. 3.6b the open-circuit voltage (V_{oc}) is dominated by temperature.

3.3.2 Calculation the PV Boost DC/DC Converter

The output voltage from PV array has small value to be synchronized with the electrical grid through the DC/AC inverter. Therefore, the DC/DC boost converter is employed to step up the output voltage of PV array in order to achieve the required voltage level, as shown in Fig. 3.7. The configuration of the DC/DC boost converter

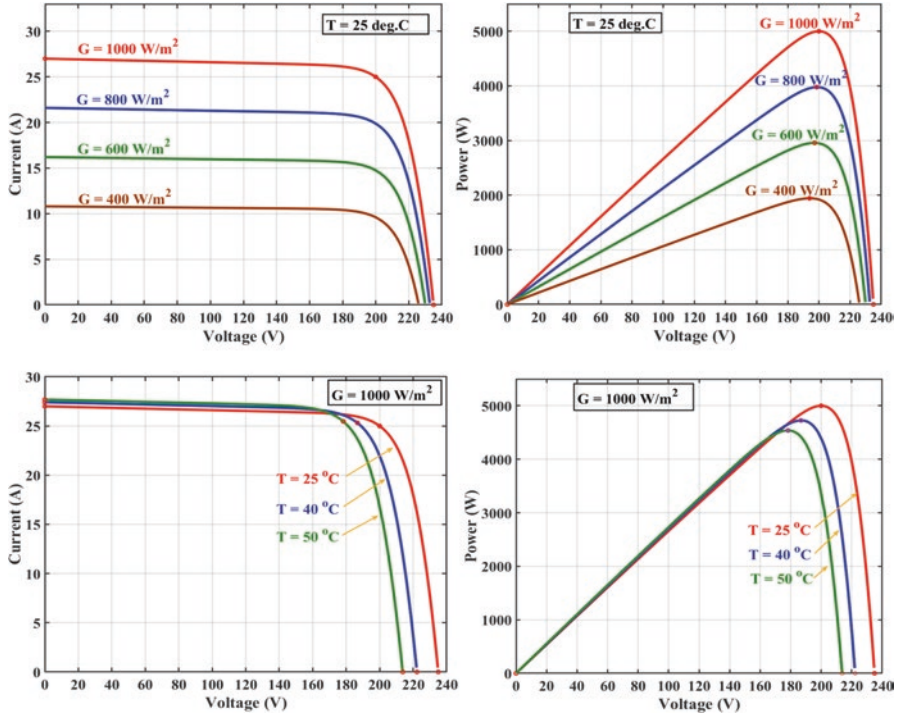


Fig. 3.6 Characteristics of a typical PV array during variation of solar irradiance and temperature. (a) Current-voltage (I-V) and power-voltage (P-V) characteristics of PV array under variable solar irradiance. (b) Current-voltage (I-V) and power-voltage (P-V) characteristics of PV array under variable temperature

includes two nearly ideal semiconductor switches such as diode and MOSFET and energy storage elements such as inductor and capacitor. The storage elements in the boost converter act as a low-pass filter to reduce the voltage ripple. An input capacitor (C_a) is employed to stabilize the terminal voltage of PV array caused by varying converter input current due to switching, while an output capacitor (C_1) acts as a low-pass filter to reduce the output voltage ripple [68].

The operation modes of the DC/DC converter are illustrated in Fig. 3.8. When the switch (Q) is turned on, current flows through the inductor (L_a) and switch (Q) in a clockwise direction, and the inductor stores some energy by generating a magnetic field ($V_{L_a} = V_{pv}$). When the switch (Q) is turned off, the magnetic field previously created will be obliterated to maintain the current flows toward the DC link, and also the polarity of the induced voltage across the inductor is reversed. Therefore, the inductor voltage (V_{L_a}) adds to the array voltage (V_{pv}), and the output voltage (V_{dc}) will be greater than the input voltage ($V_{dc} = V_{pv} + V_{L_a}$). Furthermore, the MPPT technique is implemented on the boost converter to capture the maximum power from PV array during variation of the solar irradiance. Therefore, the switching duty cycle of the boost converter (Dy) is generated by the MPPT technique.

As a PV cell is a current source, a capacitor (C_a) is estimated using Eq. (2.5) and interconnected in parallel to the output terminal of PV array, so that it can work as a voltage source to the DC/DC boost converter. The relations between input and output variables of the DC/DC boost converter and the values of its elements are expressed as follows [69]:

$$C_a = \frac{Dy * V_{PV}}{4 * \Delta V_{PV} * f_s^2 * I_{dc}} \tag{3.5}$$

$$Dy = 1 - \frac{V_{PV}}{V_{dc}} \tag{3.6}$$

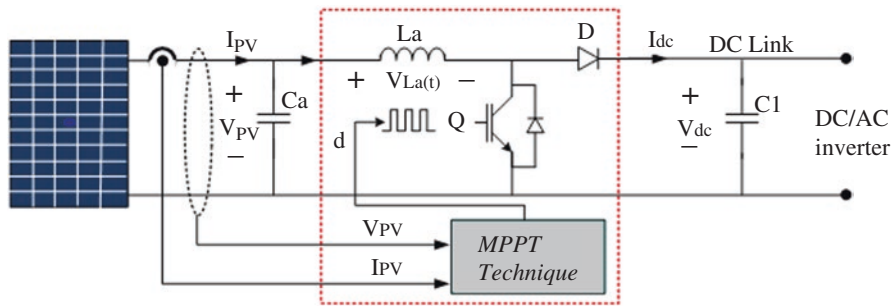


Fig. 3.7 Basic configuration of the DC/DC boost converter

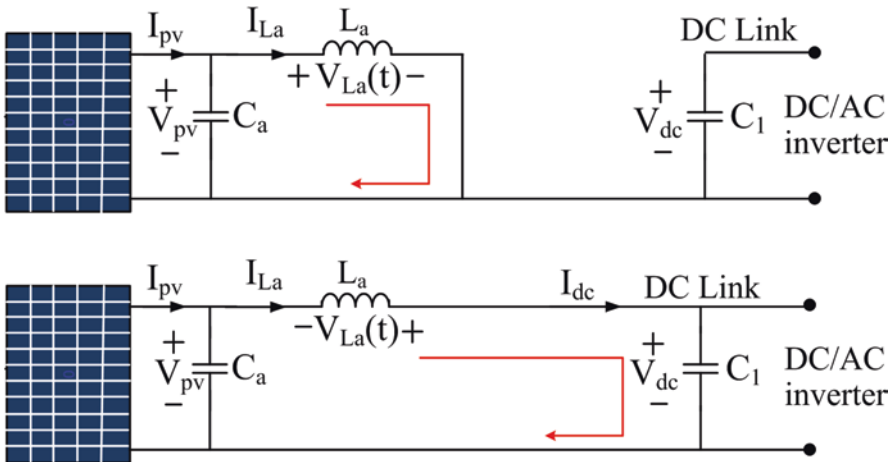


Fig. 3.8 Switching modes of the DC/DC boost converter. (a) Mode 1: when the switch (Q1) is turned on. (b) Mode 2: when the switch (Q1) is turned off

$$L_a = \frac{V_{PV} * (V_{dc} - V_{PV})}{\Delta I_{La} * f_s * V_{dc}} \quad (3.7)$$

$$\Delta I_{La} = 0.13 * I_{PV} * \frac{V_{dc}}{V_{PV}} \quad (3.8)$$

$$C_1 \geq \frac{P_{PV}}{\Delta V_0 * f_s * V_{dc}} \quad (3.9)$$

where:

V_{PV}	Is the input voltage to the converter from PV array (V)
I_{PV}	Is maximum current that the array can provide (A)
P_{PV}	Is nominal the power of the PV array (W)
f_s	Is the switching frequency (Hz)
C_a	Is the PV array link capacitance (F)
C_1	Is the DC link capacitance (F)
l_a	Is the boost converter inductor (H)
V_{dc}	Is the output voltage from the boost converter (V)
Dy	Is the duty cycle of the boost converter
ΔV_{PV}	That is the change in PV voltage (V)
ΔI_{La}	Is the ripple current of boost inductor (I)
ΔV_0	Is the ripple of output voltage (V)

3.4 MPPT Techniques of Stand-Alone PV System

The intensity of the incident solar irradiance on the PV array varies due to different reasons such as the variation of time in a day, the atmospheric effects such as clouds, and the latitude of the location. Therefore, the MPPT techniques are employed to regulate the output voltage and output current from the PV array in order to extract the maximum power during variation of the solar irradiance and enhance the overall efficiency of the grid-connected PV systems. In this section, the principle of the MPPT is a review, and simulation of two MPPT techniques implemented in the PV systems is introduced. Over the past decades, many methods to find the MPP have been developed. These techniques differ in many aspects such as required sensors, complexity, cost, the range of effectiveness, convergence speed, correct tracking when irradiation and/or temperature change, and hardware needed for the implementation or popularity, among others. Some of the most popular MPPT techniques are [14]:

1. Perturb and observe (hill climbing method)
2. Incremental conductance method

3. Fractional short circuit current
4. Fractional open circuit voltage
5. Fuzzy logic
6. Neural networks
7. Ripple correlation control
8. Current sweep
9. DC-link capacitor droop control
10. Load current or load voltage maximization
11. $\frac{dP}{dV}$ or $\frac{dP}{dt}$ feedback control

Among several techniques mentioned, the P&O method and the InCond algorithms are the most commonly applied algorithms. Other techniques based on different principles include fuzzy logic control, neural network, fractional open circuit voltage or short circuit current, current sweep, etc. Most of these methods yield a local maximum, and some, like the fractional open circuit voltage or short circuit current, give an approximated MPP, rather than an exact output. In normal conditions the V-P curve has only one maximum. However, if the PV array is partially shaded, there are multiple maxima in these curves. Both P&O and InCond algorithms are based on the “hill climbing” principle, which consists of moving the operation point of the PV array in the direction in which the power increases. Hill climbing techniques are the most popular MPPT methods due to their ease of implementation and good performance when the irradiation is constant. The advantages of both methods are simplicity and requirement of low computational power. The drawbacks are as follows: oscillations occur around the MPP, and they get lost and track the MPP in the wrong direction during rapidly changing atmospheric conditions. In the following, a review and simulation results of P&O and InCond MPPT techniques that are implemented in the PV systems are introduced.

3.4.1 *Perturb and Observe MPPT Technique*

The generated power and the output current from PV array vary nonlinearly with the array output voltage and the solar irradiance level. Therefore, it is essential to operate the PV array at the optimum voltage level (V_{MPP}) to extract the maximum power from it and increase the overall efficiency of the PV conversion systems. The maximum power point (MPP) is obtained when the gradient of power-voltage (P-V) curve is equal to zero as illustrated in Fig. 3.9. Thus, in order to track the MPP, the output voltage from PV array (V_{pv}) is regulated so that it increases when the derivative of power with respect to voltage is positive ($\frac{dP_{pv}}{dV_{pv}} > 0$), and it decreases when the derivative of power with respect to voltage is negative ($\frac{dP_{pv}}{dV_{pv}} < 0$). The control algorithm which provides continuous tracking of the MPP can be expressed as follows [70]:

$$V_{\text{MPP}} = K_1 \int \frac{dP_{\text{pv}}}{dV_{\text{pv}}} dt \quad (3.10)$$

The algorithm involves a perturbation on the duty cycle of the power converter and a perturbation in the operating voltage of the DC link between the PV array and the power converter. Perturbing the duty cycle of the power converter implies modifying the voltage of the DC link between the PV array and the power converter. In this method, the sign of the last perturbation and the sign of the last increment in the power are used to decide the next perturbation. As can be seen in Fig. 3.9, on the left of the MPP incrementing the voltage increases the power, whereas on the right decrementing the voltage decreases the power. If there is an increment in the power, the perturbation should be kept in the same direction, and if the power decreases, then the next perturbation should be in the opposite direction. Based on these facts, the algorithm is implemented as shown in the flowchart in Fig. 3.10, and the process is repeated until the MPP is reached.

The P&O algorithm is one of the most popular MPPT techniques due to its simplicity, ease of implementation, and requirement of low computational power. The algorithm involves a perturbation on the duty cycle of the DC/DC converter that implies modifying the operating voltage of the DC link between the PV array and the DC/DC converter. In the P&O MPPT technique, the sign of last perturbation and the sign of the last increment in the power are used to decide the next perturbation. Therefore, if there is an increment in the power, the next perturbation should be kept in the same direction, and if the power decreases, then the subsequent perturbation should be in the opposite direction. Based on these facts, the P&O MPPT technique can be summarized in Table 3.1 [47].

The main drawback of the P&O MPPT technique is the oscillation around the MPP instead of directly tracking it. Since, when the operating point reaches very close to the MPP, it does not stop at the MPP and keeps on perturbing in both the directions. The oscillation can be minimized by reducing the perturbation step size. However, the smaller perturbation size slows down the response of the MPPT. The

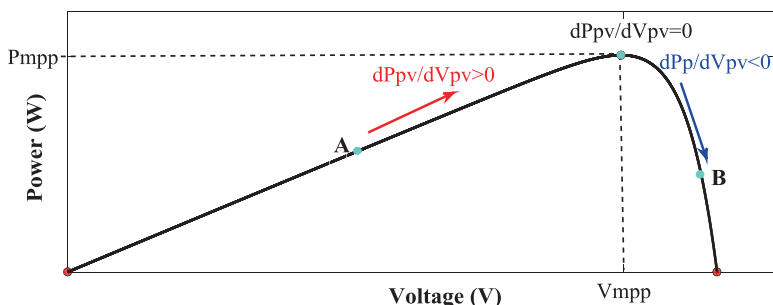


Fig. 3.9 The basic principle of MPPT in PV conversion systems

solution to this conflicting situation is to have a variable perturbation step size that

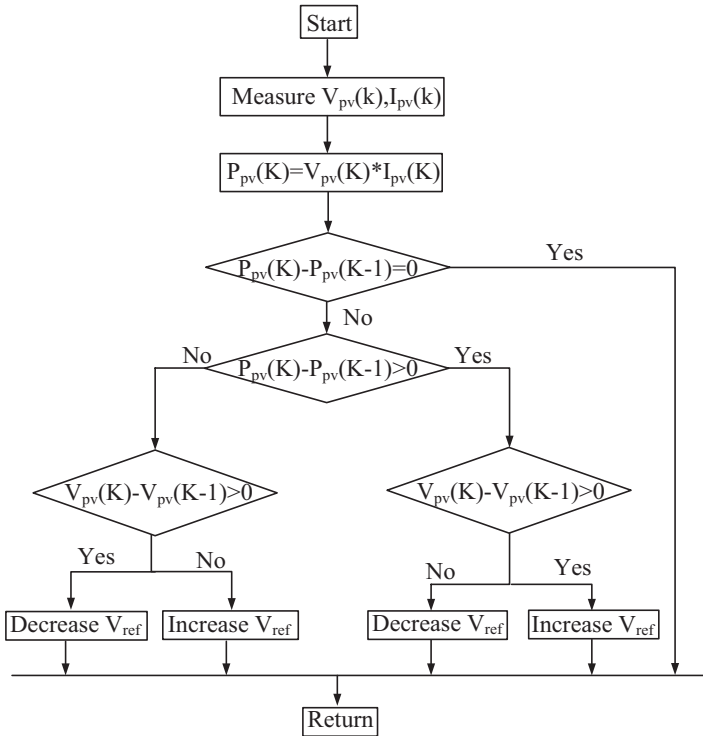


Fig. 3.10 Flow chart of the P&O MPPT technique

Table 3.1 Summary of the P&O MPPT technique

Perturbation	Change in power	Next perturbation
Positive	Positive	Positive
Positive	Negative	Negative
Negative	Positive	Negative
Negative	Negative	Positive

gets smaller toward the MPP [71]. Moreover, the P&O MPPT technique cannot track the MPP during the lower solar irradiance levels and when the solar irradiance changes rapidly. During the rapid variation of the solar irradiance, this MPPT technique considers the change in the MPP is due to perturbation and ends up calculating the MPP in the wrong direction.

3.4.1.1 Simulation Model and Results of P&O MPPT Technique

In order to verify the MPP tracker for the PV system simulation, the P&O MPPT strategy is applied at different ambient conditions to show how the proposed MPPT method can effectively and accurately track the maximum power under different. The solar irradiation and cell temperature profile are illustrated in Fig. 3.11. The detailed block diagram of the P&O algorithm mentioned above is constructed using MATLAB/SIMULINK, and the model is shown in Fig. 3.12. Here the voltage and current inputs are sensed to compute power as shown. A saturation limit is set to monitor the increase or decrease in voltage in order to avoid oscillations in the MPP.

Figure 3.13 shows the PV voltage, current, and power versus time curve without the MPPT technique at variable temperature and variable irradiation levels which are shown in Fig. 3.11. It is inferred that the output voltage obtained without MPPT technique changes its value with the change in solar irradiation and temperature. Solar irradiation varies from 600 W/m² to 1000 W/m² and drops again to 800 W/m² to be offset by the change in the value of the PV voltage 195 V and increase to 225 V and decrease again to 205 V, respectively, and the output voltage did not start from the desired value. For the current and the power did not reach its maximum value with the change of solar irradiation to be the maximum power of the PV is 4000 W instead of 5000 W at the sun irradiation value 1000 W/m² and temperature of 25 °C.

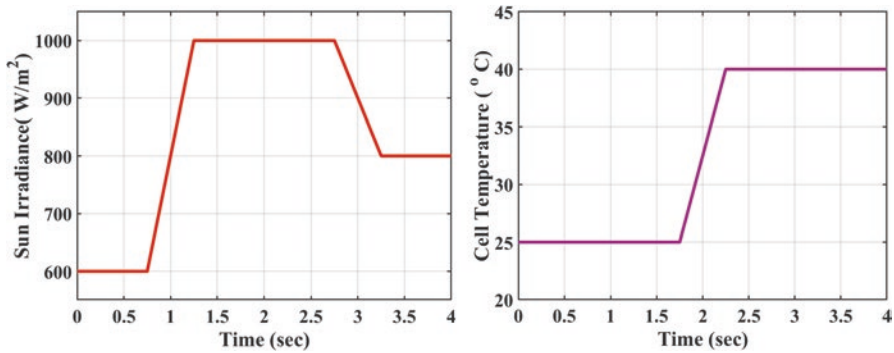


Fig. 3.11 The solar irradiation and cell temperature profile

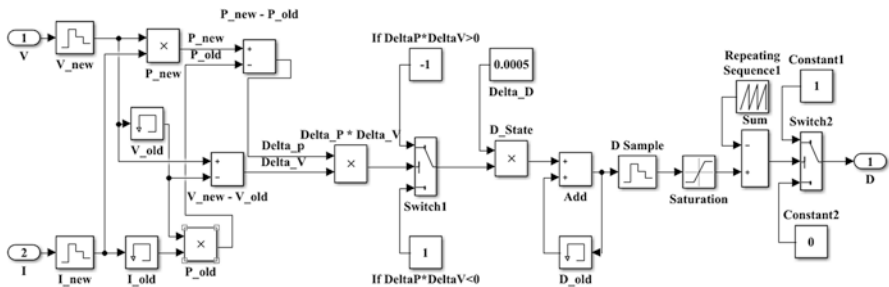


Fig. 3.12 MATLAB/Simulink model of the P&O MPPT technique

The P&O method was applied, and the output was observed as shown in Fig. 3.14 for the same profile of irradiation and temperature. As shown in Fig. 3.14, the output voltage of PV array traces the desired value well in response to the variation of the solar irradiance. When the solar irradiance is decreased from $G = 600 \text{ W/m}^2$ to $G = 1000 \text{ W/m}^2$, the MPPT controller increases the array output voltage from 200 V to 204 V and go back again to 200 V after irradiance constancy at 1000 W/m^2 in order to extract the maximum power from the PV array. Then, the MPPT controller decreases the output voltage of PV array from 200 V to 188 V, in response to the variation of temperature of PV array from $25 \text{ }^\circ\text{C}$ to $40 \text{ }^\circ\text{C}$ and change the solar irradiance from $G = 1000 \text{ W/m}^2$ to $G = 800 \text{ W/m}^2$. Therefore, the MPPT controller can accurately track the PV array voltage at the maximum power point (V_{mpp}) to harness the maximum power from the PV array during the rapid variation of solar irradiance and cell temperature. Also, Fig. 3.14 illustrates that the output current of PV array (I_{pv}) reflects the same scenario of the solar irradiance and cell temperature. When the solar irradiance is changed from $G = 600 \text{ W/m}^2$ to $G = 1000 \text{ W/m}^2$, it leads to increase the output current of PV array from 15 A to 25 A. Then, the PV array current decreases from 25 A to 20 A, in response to the change of temperature of PV

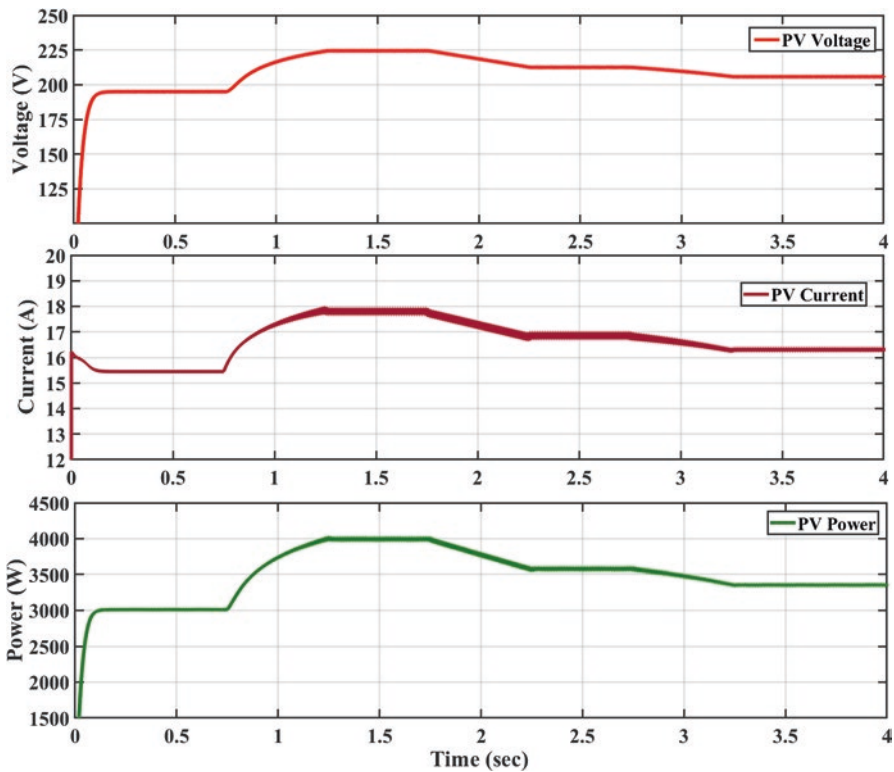


Fig. 3.13 The output of PV voltage, current, and power versus time curve without MPPT technique

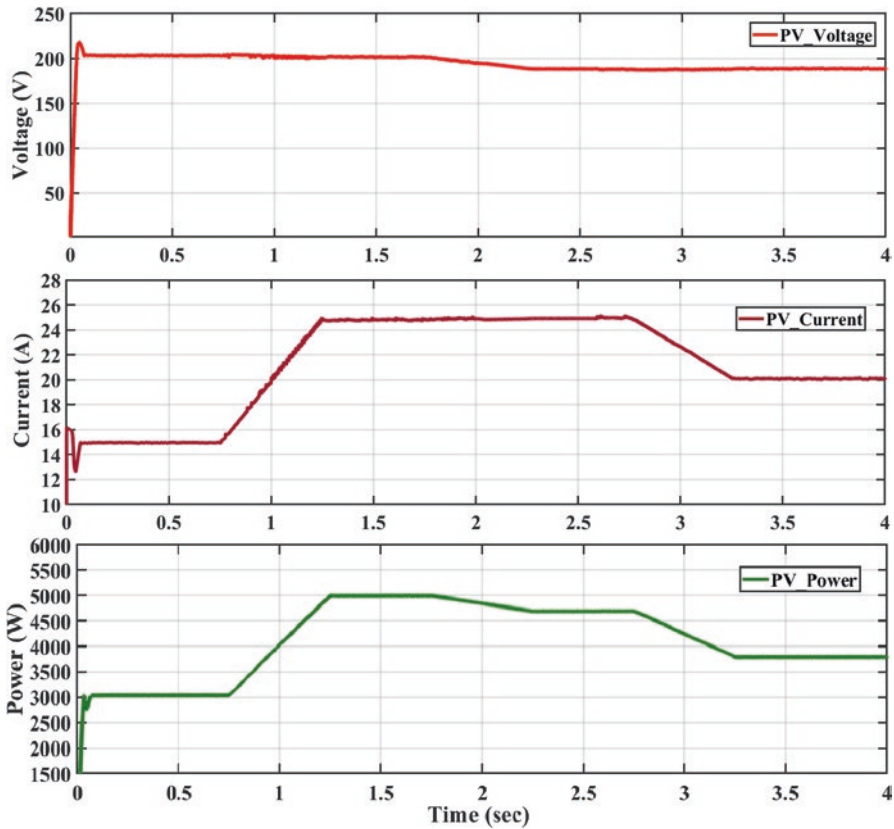


Fig. 3.14 The output of PV voltage, current, and power versus time curve with P&O MPPT technique

array from 25 °C to 40 °C and variation of the solar irradiance from $G = 1000 \text{ W/m}^2$ to $G = 800 \text{ W/m}^2$. In order to evaluate the validation of the MPPT technique, Fig. 3.14 shows the output power of one PV array (P_{pv}). It can be seen that the P&O MPPT technique can track accurately the MPP when the cell temperature and solar irradiance change rapidly; also it generates more active power as compared with the case that the MPPT technique is disabled. In all cases of change for both solar irradiation and temperature, the maximum value was obtained for both PV out current and power. Figure 3.15 shows voltage, current, and power of DC/DC boost converter which inferred that get the MPP for loads.

3.4.2 Incremental Conductance MPPT Technique

The InCond MPPT technique is widely implemented in the PV conversion systems due to its simplicity and advantage of offering good performance during the lower solar irradiance levels and when the solar irradiance changes rapidly. The InCond MPPT technique utilizes the current and voltage sensors to sense the output current and voltage of the PV array. In the InCond MPPT method, the array terminal

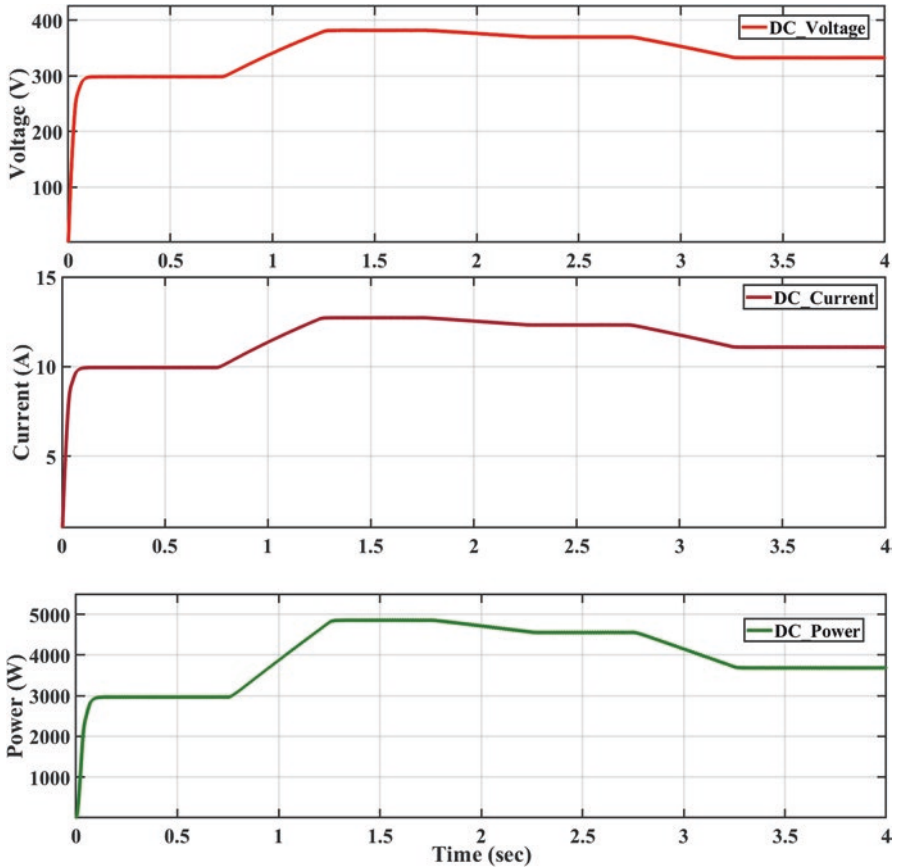


Fig. 3.15 The output DC/DC boost converter – voltage, current, and power with P&O MPPT technique

voltage (V_{pv}) is always adjusted according to the PV array voltage at MPP (V_{MPP}); it is based on the incremental and conductance of the PV array. The basic concept of the InCond MPPT technique is illustrated in Fig. 3.16.

The flow chart of this MPPT technique is shown in Fig. 3.17. The operation of InCond MPPT technique is based on the fact that the derivative of power with respect to voltage ($\frac{dP_{pv}}{dV_{pv}}$) is equal to zero at the MPP. Moreover, this derivative is positive at the left of the MPP ($\frac{dP_{pv}}{dV_{pv}} > 0$) and is negative at the right of the MPP ($\frac{dP_{pv}}{dV_{pv}} < 0$) [72]. The mathematical model of the InCond MPPT technique can be expressed as follows:

The output power from the PV array:

$$P_{pv} = V_{pv} * I_{pv} \quad (3.11)$$

$$\frac{dP_{pv}}{dV_{pv}} = \frac{d}{dV_{pv}} [V_{pv} * I_{pv}] = I_{pv} + V_{pv} \frac{dI_{pv}}{dV_{pv}} \quad (3.12)$$

Then,

$$\frac{dP_{pv}}{dV_{pv}} = 0, \frac{dI_{pv}}{dV_{pv}} = -\frac{I_{pv}}{V_{pv}} \text{ at the MPP, } \Delta V_n = 0 \quad (3.13)$$

$$\frac{dP_{pv}}{dV_{pv}} > 0, \frac{dI_{pv}}{dV_{pv}} > -\frac{I_{pv}}{V_{pv}} \text{ left of the MPP, } \Delta V_n = +\delta (\text{increment } V_{pv}) \quad (3.14)$$

$$\frac{dP_{pv}}{dV_{pv}} < 0, \frac{dI_{pv}}{dV_{pv}} < -\frac{I_{pv}}{V_{pv}} \text{ Right of the MPP, } \Delta V_n = -\delta (\text{decrement } V_{pv}) \quad (3.15)$$

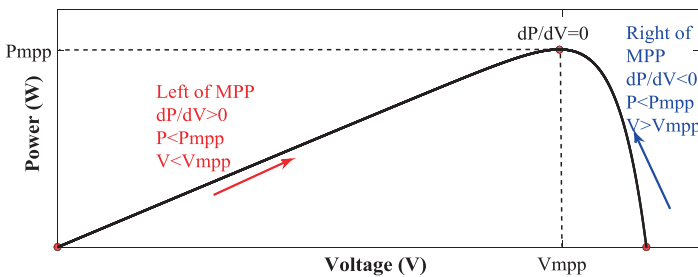


Fig. 3.16 The basic concept of InCond MPPT technique

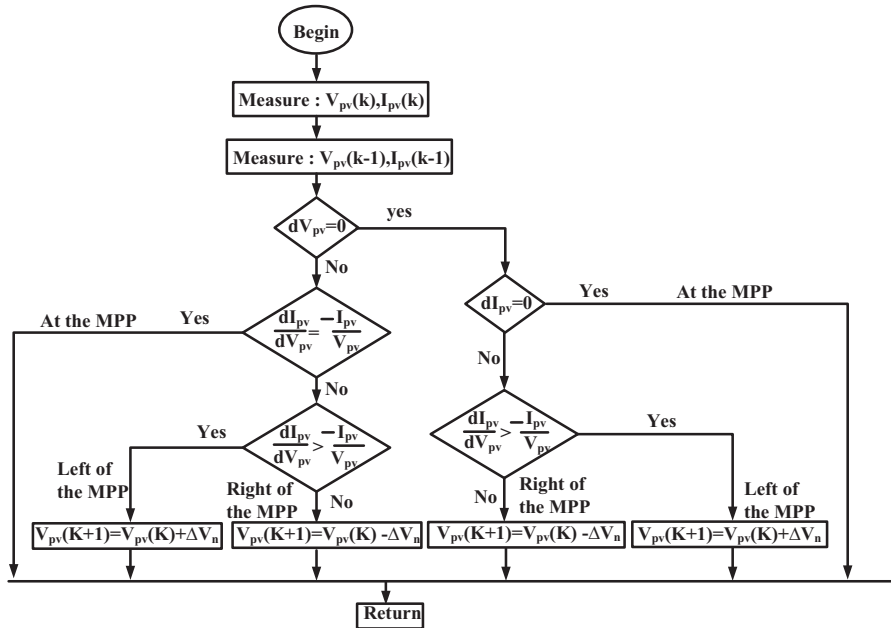


Fig. 3.17 Flow chart of InCond MPPT technique

Table 3.2 Major characteristics of the MPPT techniques

MPPT technique	PV array dependence	True MPP?	Convergence speed	Implementation complexity	Sensed parameters
P&O	No	Yes	Varies	Low	Voltage, current
InCond	No	Yes	Varies	Medium	Voltage, current

Thus, the MPP can be tracked by comparing the InCond $\left(\frac{dI_{pv}}{dV_{pv}}\right)$ with the instantaneous conductance $\left(\frac{I_{pv}}{V_{pv}}\right)$ as illustrated in the flowchart in Fig. 3.17. This algorithm increments or decrements the array terminal voltage (V_{pv}) to track the MPP during variation of the solar irradiance. The major characteristics of the presented MPPT techniques can be summarized in Table 3.2 [73].

3.4.2.1 Simulation Model and Results of InCond MPPT Technique

The MATLAB/Simulink model of the InCond MPPT strategy method is shown in Fig. 3.18. InCond is applied at the same conditions of solar irradiation and cell temperature profile which are illustrated in Fig. 3.11. In this MPPT strategy, the tracking of the MPP is obtained by regulating the terminal voltage of PV array (V_{pv}) in fixed steps ($\pm\Delta V_n$). If the operating point is the MPP, the error signal will be zero ($\Delta V_n = 0$). While, at the left of the MPP, this error signal is applied to the discrete time integrator to increase the output voltage of the PV array and track the MPP, on the other hand, at the right of the MPP, the output voltage of the PV array is decreased to follow the MPP. Therefore, it can be ensured that the output signal from the integrator is equal to the duty cycle correction (Delta-D).

Figure 3.19 illustrates the PV array response to the change in the solar irradiance and temperature. As shown in Fig. 3.19, the output voltage of PV array traces the desired value well in response to the variation of the solar irradiance. When the solar irradiance is decreased from $G = 600 \text{ W/m}^2$ to $G = 1000 \text{ W/m}^2$, the MPPT controller increases the array output voltage from 201 V to 209 V and goes back again to 201 V after irradiance constancy at 1000 W/m^2 in order to extract the maximum power from the PV array. Then, the MPPT controller decreases the output voltage of PV array from 201 V to 185 V, in response to the variation of temperature of PV array from $25 \text{ }^\circ\text{C}$ to $40 \text{ }^\circ\text{C}$ and change the solar irradiance from $G = 1000 \text{ W/m}^2$ to $G = 800 \text{ W/m}^2$. Therefore, the MPPT controller can accurately track the PV array voltage at the maximum power point (V_{mpp}) to harness the maximum power from the PV array during the rapid variation of solar irradiance and cell temperature.

Also, Fig. 3.19 illustrates that the output current of PV array (I_{pv}) reflects the same scenario of the solar irradiance and cell temperature. When the solar irradiance is changed from $G = 600 \text{ W/m}^2$ to $G = 1000 \text{ W/m}^2$, it leads to increase the output current of PV array from 15 A to 25 A. Then, the PV array current decreases from 25 A to 20 A, in response to the change of temperature of PV array from $25 \text{ }^\circ\text{C}$ to $40 \text{ }^\circ\text{C}$ and variation of the solar irradiance from $G = 1000 \text{ W/m}^2$ to $G = 800 \text{ W/m}^2$. In order to evaluate the validation of the MPPT technique, Fig. 3.19 shows the output power of one PV array (P_{pv}). It can be seen that the InCond MPPT technique can track accurately the MPP when the cell temperature and solar irradiance change rapidly; also it generates more active power as compared with the case that the MPPT technique is disabled. Figure 3.20 shows voltage, current, and power of DC/DC boost converter which inferred that get the MPP for loads.

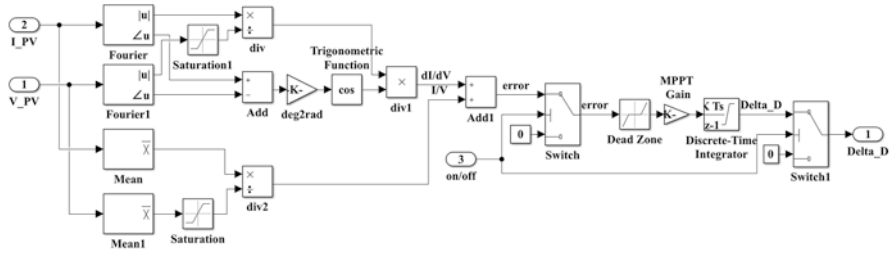


Fig. 3.18 MATLAB/Simulink model of the InCond MPPT technique

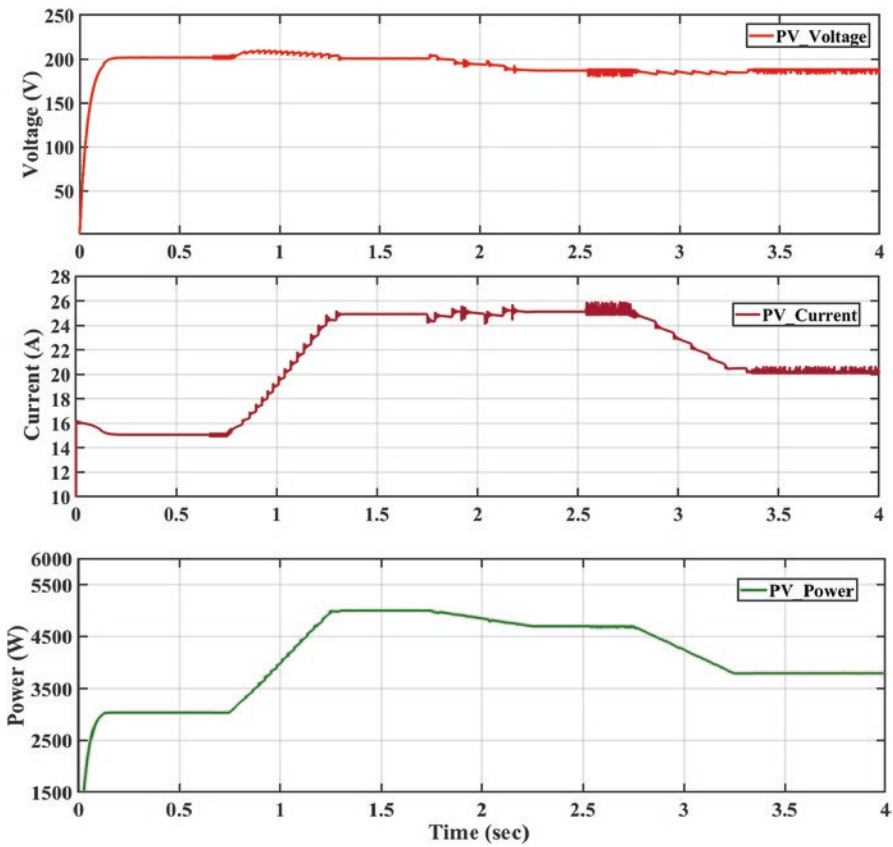


Fig. 3.19 Output of PV voltage, current, and power versus time curve with InCond MPPT technique

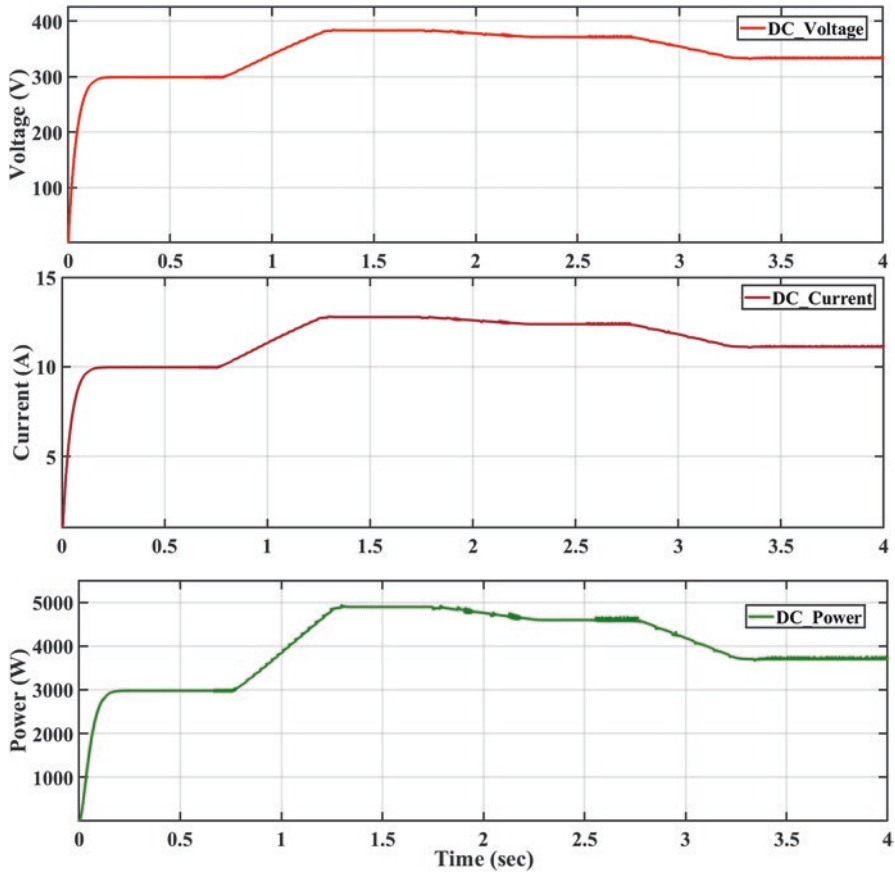


Fig. 3.20 The output DC/DC boost converter – voltage, current, and power with InCond MPPT technique

3.4.3 The Comparison Between P&O and InCond MPPT Methods

In this subsection, the simulation results of P&O and InCond MPPT techniques are compared using the same conditions. The performance of the system in terms of PV array output response of voltage, current, and power under the influence of solar irradiance change and cell temperature is compared in the cases of without using MPPT technique, using P&O MPPT technique, and using InCond MPPT technique.

Figure 3.21 illustrations of the output voltage of the PV array, with the beginning of the system work, notice that the voltage of P&O technique is reached to study state first at approximately 200 V and followed by InCond technique at the same voltage value. In the case of nonuse of the MPPT method, the voltage starts from a

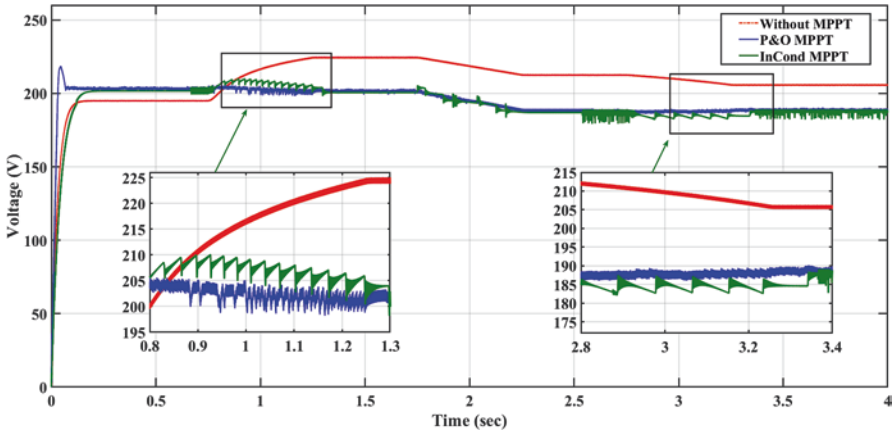


Fig. 3.21 PV array voltage comparison between P&O and InCond MPPT techniques

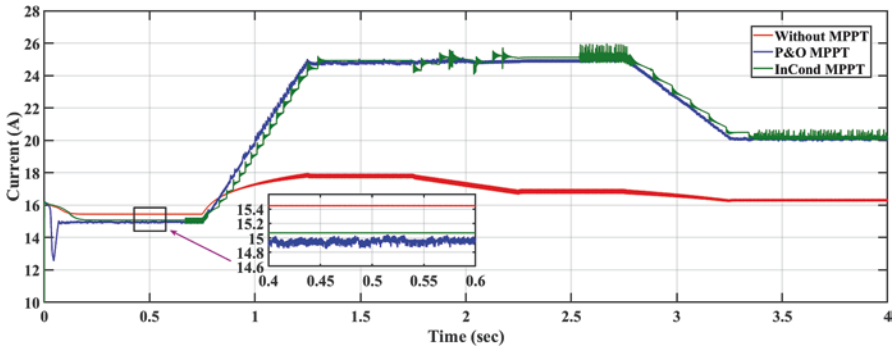


Fig. 3.22 PV array current comparison between P&O and InCond MPPT techniques

value less than the desired value (195 V). The difference between the results of the three cases is significant when a change in the value of solar irradiance occurs from $G = 600 \text{ W/m}^2$ to $G = 1000 \text{ W/m}^2$. We find that the PV output voltage of P&O technique is more stable, while the MPPT does not use the voltage to reach 225 V. The PV voltage produced by P&O and InCond MPPT technique is almost identical in the rest of the change to both solar irradiance and cell temperature.

The comparison of the PV output current in the three cases is shown in Fig. 3.22. It is clear from the figure that the current in P&O technique has more constancy and stability than the current in the InCond MPPT technique. The beginning of the system works of the PV current of P&O technique is reached to study state first at approximately 15A and followed by InCond technique at 15.1A. In the case of non-use of the MPPT method, the PV current starts from a value higher than the desired value (15.5 V). It also did not reach the maximum current when solar irradiance increased to 1000 W/m^2 .

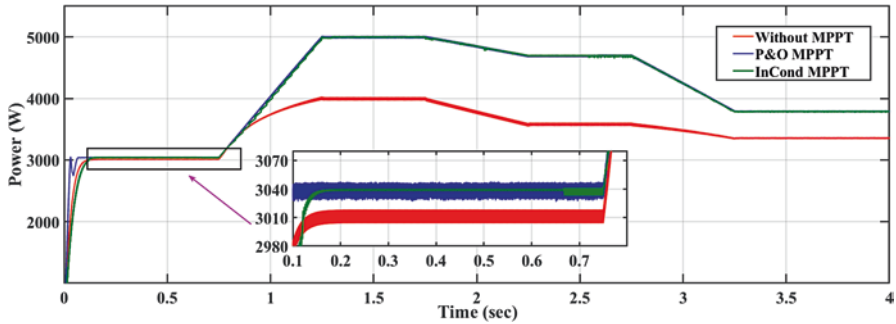


Fig. 3.23 PV array power comparison between P&O and InCond MPPT techniques

Table 3.3 PV array power under different solar irradiance and temperature

Solar irradiance level	Cell temperature	PV array power		
		With P&O MPPT	With InCond MPPT	Without MPPT
600 W/m ²	25 °C	3040 W	3040 W	3010 W
1000 W/m ²	25 °C	5000 W	5000 W	4000 W
1000 W/m ²	40 °C	4690 W	4685 kW	3585 W
800 W/m ²	40 °C	3785 W	3788 W	3355 W

The comparison of the PV output power in the two MPPT techniques is shown in Fig. 3.23. Moreover, Table 3.3 demonstrates the supply power from PV array with the P&O and InCond MPPT technique as compared with the case when the MPPT technique is disabled under different solar irradiance levels and cell temperature. It can be noticed that the power improvement is significant using the P&O InCond MPPT technique as compared with the case when the MPPT technique is disabled (fixed duty cycle of 35%).

3.5 Summary

This chapter presented the operating principle of the PV conversion systems that generate electricity via the PV effect, in which semiconductor holes and electrons are freed by photons from the incident solar irradiance. The PV systems are equipped with the DC/DC converter to implement the MPPT technique. Furthermore, this chapter introduced a review of two MPPT techniques that are implemented in the PV systems. The P&O MPPT technique and InCond MPPT technique are the most commonly implemented PV conversion systems due to its simplicity and advantage of offering good performance when the solar irradiance changes rapidly. The two MPPT techniques were simulated by the MATLAB/Simulink, and the results response of the PV array from voltage, current, and power are compared to the effect of solar irradiation and temperature change.